Available online at www.sciencedirect.com
SCIENCE DIRECT
Cancer Letters 235 (2006) 239–247
CANCER Letters
www.elsevier.com/locate/canlet

Detection of caspase-3 activation in single cells by fluorescence resonance energy transfer during photodynamic therapy induced apoptosis

Yunxia Wu, Da Xing*, Shiming Luo, Yonghong Tang, Qun Chen

Institute of Laser Life Science, South China Normal University, Guangzhou 510631, China

Received 30 October 2004; received in revised form 12 March 2005; accepted 17 April 2005

Abstract

In many apoptosis pathways, activation of caspase-3 is considered the final stage. In this study, we studied PDT induced caspase-3 activation with fluorescence resonance energy transfer (FRET) technique. A recombinant caspase-3 substrate, SCAT3, was used as the FRET probe. FRET fluorescence images were collected after PDT or TNF-α induced apoptosis. By analyzing the dynamic changes of FRET fluorescence, the results indicate that the caspase-3 activation started immediately after the PDT treatment. In contrast, FRET disruption caused by caspase-3 activation started at 3 h after TNF-α treatment, due to different signaling pathway. The results have proofed, for the first time, that FRET is a sensitive technique that can be used to investigate PDT-induced activation of caspase-3 in real-time and in single cells. By choosing appropriate recombinant substrates as FRET probes, it is likely that FRET technique will provide a new real-time means to study the mechanism of PDT at single cell level.

Keywords: Apoptosis; Caspase-3; Fluorescence resonance energy transfer; Photodynamic therapy; TNF-α

1. Introduction

Photodynamic therapy (PDT) is a new cancer treatment modality. Certain photosensitizing drugs can accumulate preferentially in lipophilic cell organelles, including mitochondria, endoplasmic reticulum, nucleus, and lysosomal membranes. The drug accumulated in the target tissue is activated by light of appropriate wavelengths [1–3]. Light activation of the drug induces formation of reactive oxygen species (ROS). The intermediates are capable to produce cellular damages that ultimately lead to cell death by either necrosis [4–7], or, apoptosis [8–15]. The production of ROS by PDT may also promote tissue destruction in part by vascular occlusion leading to ischemic necrosis [16].

Abbreviations: PDT, photodynamic therapy; ROS, reactive oxygen species; FRET, fluorescence resonance energy transfer; ECFP, enhanced cyan fluorescence protein; EYFP, enhanced yellow fluorescence protein; TNF-α, tumor necrosis factor-α; HpD, hematoporphyrin derivative; Cl^-, chloride ion; H^+, proton.

* Corresponding author. Tel.: +86 20 8521 0089; fax: +86 20 8521 6052.
E-mail address: xingda@scnu.edu.cn (D. Xing).

0304-3835/$ - see front matter © 2005 Elsevier Ireland Ltd. All rights reserved.
doi:10.1016/j.canlet.2005.04.036

Apoptosis is a very important cellular event that plays a key role in pathogeny and therapy of many diseases [17,18]. The mechanisms of the initiation and regulation of apoptosis are complex and diverse [19]. In many apoptosis pathways, activation of the effector caspases is considered the final step [20]. Among the spectrum of various caspases, caspase-3 is believed to be the primary executioner of apoptosis. With inhibition of caspase-3 activation, cell apoptosis can be blocked [21]. When caspase-3 is activated, depending on the activation mechanism, it can induce chromatin condensation, DNA fragmentation, and cleavage of the DNA repair enzyme poly (ADP-ribose) polymerase (PARP) [22]. Because the caspases-3 activation is a landmark event in apoptosis, assaying caspases-3 has been widely used as a tool for detecting programmed cell death [23]. Caspase-3 activation is typically studied by western blotting or caspase-3 activation detection kits [24,25]. Unfortunately, these techniques are time consuming and cannot be used to monitor the activation of caspases in real-time. Furthermore, the conventional detection techniques cannot be used to investigate the caspase-3 activation at single cell level.

The fluorescence resonance energy transfer (FRET) is a process by which transfer of energy occurs from a donor fluorophore molecule to an acceptor fluorophore molecule in close proximity. The emission spectrum of the donor molecule overlaps with the absorption spectrum of the acceptor molecule. When the two fluorophores are spatially close enough there is energy transfer between the donor and acceptor molecules. The excited donor transfers its energy to the acceptor. This results in a reduction in donor fluorescence emission and, at the same time, an increase in acceptor fluorescence emission [26]. FRET technique has been used widely to study protein–protein interaction in living cells [26–28]. Miura et al. [29] has constructed a FRET probe, SCAT3 that consists of a donor (enhanced cyan fluorescent protein, ECFP) and an acceptor (Venus, a mutant of yellow fluorescent protein). The linking sequence contains a caspase-3 cleavage, DEVD [30]. The activation of caspase-3 leads to the cleavage of the linker, thus, effectively reduces the FRET. Using FRET technique based on SCAT3, the spatial-temporal dynamics of caspase-3 activity in individual living cells can be monitored in real-time [29].

PDT induced caspase-3 activation has been reported by Grancille et al. [31] with conventional western blotting technique. In this work, we used SCAT3 as a FRET probe to study the caspase-3 activation in SCAT3-expressing human lung adenocarcinoma cell line (ASTC-a-1) during photosensitization-induced apoptosis. The objective of the study was to further the investigation of PDT induced caspase-3 activation in real-time, using FRET technique, within single cells.

2. Material and methods

2.1. Cell line

The human lung adenocarcinoma cell line (ASTC-a-1) was obtained from Department of Medicine, Jinan University and cultured in RM1640 supplemented with 10% fetal calf serum (FCS), penicillin (100 units/ml), and streptomycin (100 μg/ml) in 5% CO2, 95% air at 37 °C in humidified incubator.

For the FRET experiments, ASTC-a-1 cells were transfected with 1 μg plasmid DNA of SCAT3 and 10 μl of Lipofectin reagent (GIBCO) per 100 μl of serum-free medium at 37 °C for 8 h. The cells stably expressing SCAT3 reporter were screened with 0.8 mg/ml G418, and positive clones were picked up with micropipettes. SCAT3 reporter was constructed by fusing of an ECFP and a Venus with a specialized linker that contains a caspase-3 recognition and cleavage sequence (DEVD) [29]. For all treatment and imaging process, as described in the following sections, the cells were maintained at 37 °C using a Thermo Plate (Tokhi Hit, Japan) in the experiment process.

2.2. PDT and tumor necrosis factor-α treatment

SCAT3-expressing ASTC-a-1 cells (0.8×10^5) were cultured on grass-bottomed 35 mm Petri dishes in 1 ml RM1640 supplemented with 10% FCS medium for 24 h to let them attach firmly.

To detect apoptosis induced by PDT, cells were co-incubated in the dark with 16 μg/ml hematoporphyrin derivative (HpD, Beijing Institute of Pharmaceutical Industry) for 20 h before light irradiation. For the control group, cells were incubated in the same medium without HpD before irradiation. The light

source was a He–Ne laser (HN-1000, Guangzhou, China; 632.8 nm). The cells were irradiated with a fluence of 10 J/cm^2 at a fluence rate of 10 mW/cm^2.

As a parallel study to confirm and compare the caspase-3 detection in our experiments, a separate batch of cells were exposed to 150 ng/ml TNF-α a well established protocol to induce apoptosis.

2.3. Confocal and FRET image analysis

To identify the spatial distribution of SCAT3 within cells, its fluorescence images (530 nm) were collected with a confocal microscope (MRC-600, BIO-RAD) with a 60× water-immersed objective and a 510 nm long-pass filter. To match the Venus excitation wavelength, a 10 mM Argon-ion laser with 488 nm output was used. The cells were scanned in the transversal direction with 2 μm steps.

To investigate the temporal profile of caspase-3 activation in single cells after PDT or TNF-α treatment, SCAT3-expressing ASTC-a-1cells were treated with PDT or TNF-α as described above. During the treatments, the cellular fluorescent images were collected with a Nikon fluorescent microscope (ECLIPSE E600) equipped with a mercury lamp for excitation (400–440 nm) and a 455 nm dichroic mirror. The Venus and ECFP images were collected with band-filters of 510–560 and 460–490 nm, respectively. The images were recorded using a digital camera (Nikon, Tokyo, Japan) with 1280× 960 pixels resolution. Fluorescence intensities of ECFP and Venus were analyzed using the UTHSCSA ImageTool software (http://ddsdx.uthscsa.edu/dig/).

2.4. Spectral analysis

After SCAT3-expressing ASTC-a-1 cells were treated with PDT, they were re-suspended in PBS and used for fluorescence spectral analysis (LS-55, Perkin Elmer. Excitation wavelength: 433 nm. Excitation and emission splits: 10 and 15 nm, respectively). The experiment was conducted at room temperature.

2.5. Confirmation of cell apoptosis

To assess the changes in nuclear morphology typical of apoptosis, ASTC-a-1 cells were cultured on 35 mm glasses bottomed dishes. At 6 h after PDT, the cells were washed twice with phosphate-buffered saline (PBS, pH 7.4). Subsequently, the cells were stained with 1 μM Hoechst 33342 for 15 min at room temperature. The cells were then washed twice with PBS and visualized under a Nikon fluorescent microscope with a 330–380 nm band pass excitation filter and a 450–490 nm band pass emission filter.

To assess cytotoxicity of PDT, ASTC-a-1 cells were cultured in RM1640 supplemented with 10% FCS at a density of 1×10^3 cells/well in 96-well microplate for 24 h. The cells were then co-incubated with 16 μg/ml HpD for 20 h at 37 °C in the dark. The cells were then divided into six groups and exposed to He–Ne laser irradiation at fluence of 0 (control), 1, 5, 10, 15 and 20 J/cm^2, respectively. After the irradiation, the cells were cultured for an additional 24 h at 37 °C in the dark. Cytotoxicity assay was then performed with Cell Counting Kit-8 (Dojindo Laboratories, Kumamoto, Japan). The absorbance value at 450 nm, OD_{450}, was read with a 96-well plate reader (DG5032, Hua dong, Nanjing, China). The OD_{450} value is proportional inversely to the degree of cell apoptosis.

2.6. Statistical analysis

Statistical analysis was performed with the Student's paired *t*-test. Differences were considered statistically significant at $P<0.05$.

3. Results

3.1. Intracellular distribution and FRET efficiency of SCAT3

In order to detect the intracellular distribution of SCAT3 in the stably transfected ASTC-a-1 cells,

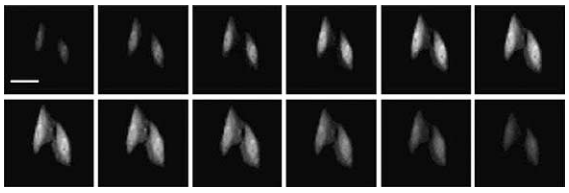

Fig. 1. Transverse-imaging series of the intracellular distribution of SCAT3 in stably transfected ASTC-a-1 cells. The scanning was performed from top to bottom of the cells, with steps of 2 μm. Scale bar = 10 μm.

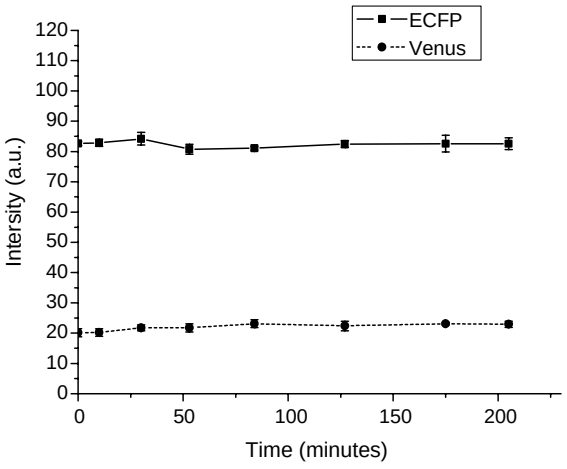

Fig. 2. The stability of FRET efficiency of SCAT3 in the stable transferred cells. The SCAT3-expressing ASTC-a-1 cells were exposed to room air and kept at 37 °C for 200 min (mean ± SD, $n = 4$).

the fluorescence of SCAT3 was collected by a confocal microscope. Venus fluorescence was observed in both cytoplasm and nucleus (Fig. 1). Venus fluorescence was more intense in nucleus than in cytoplasm, likely a result of higher expression of SCAT3 in nucleus. It has been reported that procaspase-3 localizes in the cytoplasm, caspase-3 activation is initiated firstly in the cytosol and the activated caspase-3 redistributes to the nuclear compartment [24,29]. Therefore, using this plasmid, SCAT3, the process of activated caspase-3 may be monitored in the entire cell.

SCAT3 is designed specifically to detect caspase-3 activation. The fluorescence intensity ratio between Venus and ECFP emission is directly related to the caspase-3 activity. In a control experiment, the SCAT3-expressing ASTC-a-1 cells were exposed to room air at 37 °C for various time periods up to 200 min. A time-course of fluorescence intensities of Venus and ECFP from SCAT3-expressing cells is showed Fig. 2. From the graph, the average fluorescence intensities of Venus and ECFP remained unchanged throughout the observation period. The results indicate that, there was neither change in resonance energy transfer nor photobleaching during the process. This demonstrates that, without external effects (PDT or TNF-α, in this study), FRET effect was stable and caspase-3 was not activated.

3.2. Real-time detection of caspase-3 activation in living ASTC-a-1 cells during TNFα-induced apoptosis

To validate the FRET technique, we have determined the dynamics of caspase-3 activity during TNF-α induced apoptosis. The typical time-course images of Venus and ECFP from two neighboring SCAT3-expressing cells are showed in Fig. 3. The fluorescence intensity of Venus decreased while that of ECFP increased. This can be explained by the activation of caspase-3 in the stably transected ASTC-a-1 cells. Fig. 4 shows the temporal profile of ECFP/Venus emission ratio, as measured in a single cell. After the administration of TNF-α (time 0), the ECFP/Venus ratio remained at its baseline for approximately 215 min. The ratio then increased gradually, as a result of decreased resonance energy transfer due to the cleavage of the SCAT3. The ECFP/Venus ratio reached its maximum within 90 min, suggesting all of the caspase-3 substrates were cleaved within this period. Morphologically, the cells began to show shrinkage and bleb of their membrane at 400 min after the cells were exposure to TNF-α. It is evident that caspase-3 was activated preceding cell apoptosis.

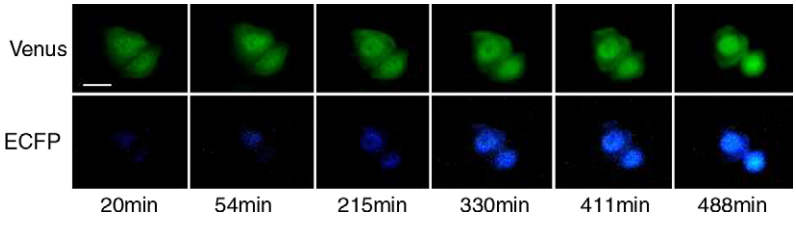

Fig. 3. Image Series of ECFP and Venus in SCAT3-expressing ASTC-a-1 cells after TNF-α treatment. Scale bar = 10 μm.

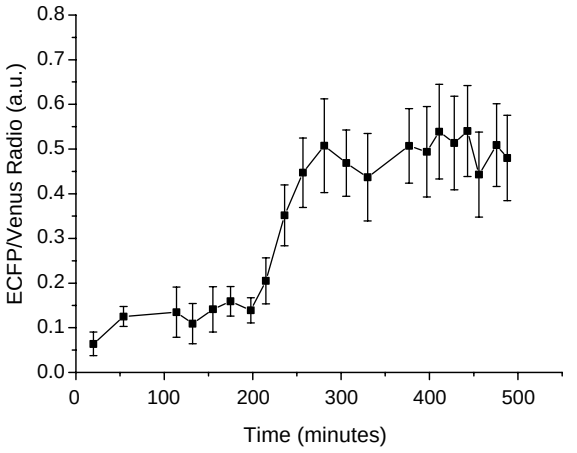

Fig. 4. Temporal profile of the Venus/ECFP emission ratio in SCAT3-expressing ASTC-a-1 cells. The cells were exposed to 150 ng/ml TNF-α (mean ± SD, $n = 4$).

3.3. Photodynamic therapy induced apoptosis in ASTC-a-1 cells

To establish a proper light dose of PDT to induce apoptosis, ASTC-a-1 cells were incubated with 16 μg/ml HpD and subsequently irradiated with various light fluence. Cells apoptosis was analyzed using Cell Counting Kit-8. The OD_{450} value, an indicator of cell apoptosis, was measured. As shown in Fig. 5A, the OD_{450} value was statistically significantly lower for cells irradiated with even 5 J/cm^2 (student's paired t-test, $P < 0.001$), and continued to decrease as the irradiation fluence increased. At 10 J/cm^2, with Hoechst 33342 staining confirmed, morphologically, that the PDT treatment induced apoptosis (Fig. 5B). Therefore, this PDT treatment protocol (16 μg/ml HpD, 10 J/cm^2 of 632.8 nm light) was chosen for further experiments.

3.4. Real-time detection of caspase-3 activation in living ASTC-a-1 cells during PDT-induced apoptosis

By using the PDT treatment protocol that induced apoptosis, as determined in the previous experiment, we next used the FRET technique to monitor the activation of caspase-3 in SCAT3-expressing ASTC-a-1 cells. The cells treated with light irradiation alone, but without photosensitizer, were considered as a control group. Fig. 6 is representative time-course images of Venus and ECFP from two neighboring cells after the PDT treatment. After the PDT treatment, the intensity of ECFP fluorescence increased while that of Venus decreased. Compared to the light irradiation only control group, ECFP/Venus ratio of the cells increased immediately after the PDT treatment. At about 100 min after PDT treatment, the ECFP/Venus ratio reached its maximum due to complete exhaustion of the SCAT3 probe. These results demonstrate that the intracellular caspase-3 was activated by certain upstream factors to cleave the linker of SCAT3, DEVD, thus disrupted the FRET during PDT-induced apoptosis (Fig. 7). The cells showed typical early apoptotic cell death morphology, such as nuclei condensation.

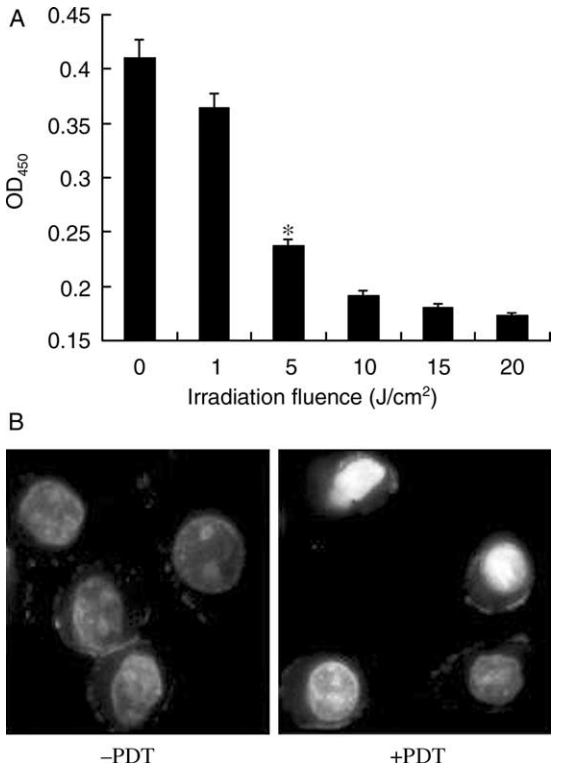

Fig. 5. PDT-induced apoptosis in ASTC-a-1 cells. (A) Changes in cell viability induced by PDT (means ± SD, $n = 4$) (Student's T tests: 0 vs. 5 J/cm^2, $^*P < 0.001$). (B) Hoechst 33342 staining of cells 6 h after PDT treatment. Scale bar = 10 μm.

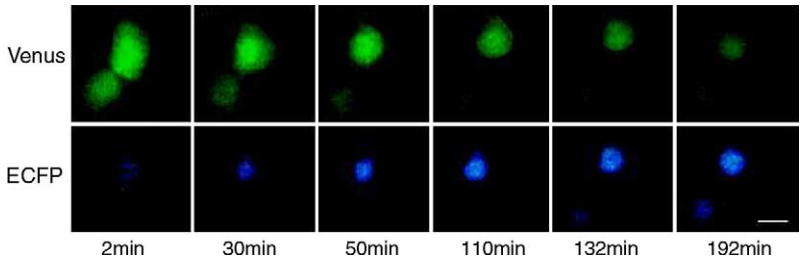

Fig. 6. Image series of caspase-3 activation in SCAT3-expressing ASTC-a-1 cells after PDT treatment. Scale bar = 10 μm.

3.5. Spectral analysis of SCAT3-expressing ASTC-a-1 cells during PDT-induced apoptosis

To further confirm the disruption of FRET in SCAT3-expressing cells after PDT treatment, the emission spectra of the cell suspension were measured (Fig. 8). Before PDT treatment, bimodal emission peaks at 480 and 530 nm were observed with 433 nm excitation. The strong 530 nm peak of ECFP was due to the occurrence of FRET. Four hours after the PDT treatment, caspase-3 was activated, the peak at 530 nm disappeared and the peak of 480 nm appeared. This observation is a result of SCAT3 site (DEVD) was cleaved by caspase-3 and the FRET between Venus to ECFP was disrupted.

4. Discussion

The present report demonstrates that FRET technique can be used monitor caspase-3 activation at single cell level in real-time. Caspase-3 is activated during PDT induced apoptosis that is confirmed by secondary techniques, i.e. Hoechst 33342 staining.

Photodynamic therapy employs a combination of a photosensitizing chemical and visible light to produce singlet oxygen and other ROS [30,32], and these ROS can cause mitochondrial damage and induce apoptosis through release of cytochrome *c* and activation of caspase-3 [22]. Caspase-3 is the most common executioner caspase and is essential for the terminal stage of apoptosis in many cases [22]. It is required for DNA fragmentation and morphological changes in apoptosis [33]. The precursor form of caspase-3 is predominantly synthesized in the cytosol [33–35], and activated caspase-3 can be translocated from the cytosol into the nucleus [30,36].

SCAT3 is an established caspase-3 specific recombinant FRET probe [22]. It is insensitive to changes in Cl^- and H^+ [30]. Our data indicate that SCAT3 can express in both cytoplasm and nucleus. Furthermore, the results show that, un-interrupted FRET signal of SCAT3 in room air is stable for a minimum of 3 h and is insensitive to light irradiation alone, making it an ideal choice for studying caspase-3 activation during PDT.

Our results show that, caspase-3 activation occurred 3 h after the administration of TNF-α that consequently induced apoptosis. The observation is comparable to that reported by Miura et al. with a different cell line [29]. This firstly validated the effectiveness of our FRET experimental apparatus. More importantly, by comparing the temporal profiles of FRET from our TNF-α and PDT studies, we have noticed that there was a significant time difference for caspase-3 activation induced by the two treatments.

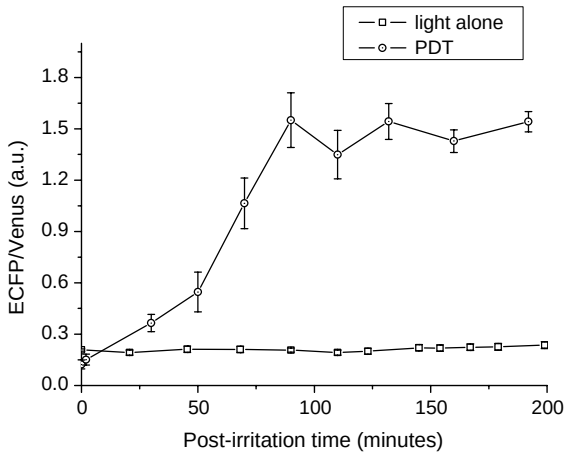

Fig. 7. Temporal profiles of the Venus/ECFP emission ratio for SCAT3-expressing ASTC-a-1 cells with PDT treatment and light irradiation alone (no photosensitizer) (mean ± SD, $n = 4$).

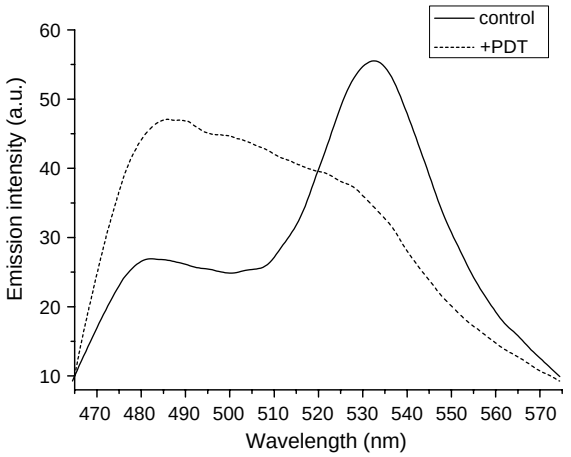

Fig. 8. Fluorescence spectra of SCAT3-expressing ASTC-a-1 cells. Solid line, control; Dash line, 4 h after PDT treatment.

The apoptosis pathway stimulated by TNF-α involves activation of death receptors and caspase-8 as initiator [37], while apoptosis by PDT is mainly through the mitochondria pathway and has caspase-9 as its initiator [38]. The difference in the pathways is likely the reason to cause the activation of caspase-3 to occur more rapidly in PDT than that with TNF-α treatment. This indicates that FRET can be a sensitive means for studying caspase-3 activation for different pathways.

FRET, a noninvasive technique, can spatio-temporally monitor cellular events in physiological condition at single cell level [39–41]. It has been utilized to study enzyme activity, protein location, protein translocation, small ligand binding, protein–protein interaction, conformational change, and posttranslational modification in real-time, as reviewed by Gaits et al. [28]. Specifically, FRET has been used to detect apoptotic signals that involve activation of different caspases [20,23,30,42], interactions between Bcl-2 and Bax [39,40,43–45], Ca^{2+} levels [41,46,47] and etc. In the present study, we have shown, for the first time, that the activation of caspase-3 during PDT-induced apoptosis can be monitored by FRET.

In conclusion, we have found that apoptosis can be induced with PDT in human lung adenocarcinoma cells. With a recombinant FRET probe SCAT3, we have determined that caspase-3 was activated during the PDT induced apoptotic process. By choosing appropriate recombinant substrates as FRET probes, it is likely that FRET technique will provides a new real-time means to study the mechanism of PDT at single cell level.

Acknowledgements

We thank Dr Masayuki Miura of RIKEN Brain Science Institute for generously providing the SCAT3 used in the experiments; Ying Jin and Jinjun Wang for technical assistance.

This research is supported by the National Natural Science Foundation of China (60378043; 30470494), and the Natural Science Foundation of Guangdong Province (015012; 04010394)

References

[1] M. Geze, P. Morliere, J.C. Maziere, K.M. Smith, R. Santus, Lysosomes, a key target of hydrophobic photosensitizers proposed for photochemotherapeutic applications, J. Photochem. Photobiol. 20 (1993) 23–35.
[2] T.J. Dougherty, C.J. Gomer, B.W. Henderson, G. Jori, D. Kessel, M. Korbelik, et al., Photodynamic therapy: review, J. Natl Cancer Inst. 90 (1998) 889–902.
[3] I.J. Macdonald, T.J. Dougherty, Basic principles of photodynamictherapy, J. Porphyrins Phthalocyanines 5 (2001) 105–129.
[4] H.I. Pass, Photodynamic therapy in oncology: mechanisms and clinical use, J. Natl Cancer Inst. 85 (1993) 443–456.
[5] C.J. Lightdale, S.K. Heier, N.E. Marcon, J.S. McCaughan, H. Gerdes, B.F. Overholt, et al., Photodynamic therapy with porfimer sodium versus thermal ablation therapy with Nd:YAG laser for palliation of esophageal cancer: a multicenter randomized trial, Gastrointest. Endosc. 42 (1995) 507–512.
[6] H. Kato, T. Okunaka, H. Shimatani, Photodynamic therapy for early stage bronchogenic carcinoma, J. Clin. Laser Med. Surg. 14 (1996) 235–238.
[7] M. Ochsner, Photophysical and photobiological processes in the photodynamic therapy of tumours, J. Photochem. Photobiol. 39 (1997) 1–18.
[8] J.P. Thomas, R.D. Hall, A.W. Girotti, Singlet oxygen intermediacy in the photodynamic action of membrane-bound hematoporphyrin derivative, Cancer Lett. 35 (1987) 295–302.
[9] M.L. Agarwal, M.E. Clay, E.J. Harvey, H.H. Evans, A.R. Antunez, N.L. Oleinick, Photodynamic therapy induces rapid cell death by apoptosis in L5278Y mouse lymphoma cells, Cancer Res. 51 (1991) 5993–5996.
[10] M. Geze, P. Morliere, J.C. Maziere, K.M. Smith, R. Santus, Apoptosis during photodynamic therapy—induced ablation of RIF-1 tumors in C3H mice: electron microscopic, histopathologic and biochemical evidence, J. Photochem. Photobiol. 58 (1993) 771–776.

[11] M.L. Agarwal, H.E. Larkin, S.I.A. Zaidi, H. Mukhtar, N.L. Oleinick, Phospholipase activation triggers apoptosis in photosensitized mouse lymphoma cells, Cancer Res. 53 (1993) 5897–5902.
[12] S.I. Zardi, N.L. Oleinick, M.T. Zain, H. Mukhtar, Apoptosis during photodynamic therapy-induced ablative RIF-1 tumors in C3H mice, Photochem. Photobiol. 58 (1993) 771–776.
[13] Y. Xiao-Yan, R.A. Sikes, S. Thomsen, L.W.K. Chung, S.L. Jacques, Photodynamic therapy with Photofrin II induces programmed cell death in carcinoma cell lines, Photochem. Photobiol. 59 (1994) 468–473.
[14] Y. Luo, C.K. Chang, D. Kessel, Rapid initiation of apoptosis by photodynamic therapy, Photochem. Photobiol. 63 (1996) 528–534.
[15] J. He, M.L. Agarwal, H.E. Larkin, L.R. Friedman, L.-Y. Xue, N.L. Oleinick, The induction of partial resistance to photodynamic therapy by the proto-oncogene BCL-2, Photochem. Photobiol. 64 (1996) 845–852.
[16] T.H. Foster, R.S. Murant, R.G. Bryant, R.S. Knox, S.L. Gibson, R. Hilf, Oxygen consumption and diffusion effects in photodynamic therapy, Radiat. Res. 126 (1991) 296–303.
[17] A. Ashkenazi, V.M. Dixit, Death receptors: signaling and modulation, Science 281 (1998) 1305–1308.
[18] S. Nagata, Apoptosis by death factor, Cell 88 (1997) 355–365.
[19] F. Wang, T. Chen, D. Xing, Measuring dynamics of caspase-3 activity in living cells using FRET technique during apoptosis induced by high fluence low power laser irradiation, Lasers Surg. Med. 36 (2005) 2–7.
[20] M. Rehm, H. Dussmann, R.U. Janicke, J.M. Tavare, D. Kogel, J.H.M. Prehn, Single-cell fluorescence resonance energy transfer analysis demonstrates that caspase activation during apoptosis is a rapid process, J. Biol. Chem. 227 (2002) 24506–24514.
[21] M. Lam, N.L. Oleinick, A.L. Nieminen, Photodynamic therapy-induced apoptosis in epidermoid carcinoma cells, J. Cell Biol. 276 (2001) 47379–47386.
[22] L. Xue, S. Chiu, N.L. Oleinick, Photodynamic therapy-induced death of MCF-70 human breast cancer cells: a role for caspase-3 in the late steps of apoptosis but not for the critical lethal event, Exp. Cell Res. 263 (2001) 145–155.
[23] K.Q. Luo, V.C. Yu, Y. Pu, D.C. Chang, Application of the fluorescence resonance energy transfer method for studying the dynamics of caspase-3 activation during UV-induced apoptosis in living HeLa cells, Biochem. Biophys. Res. Commun. 283 (2001) 1054–1060.
[24] M. Mahitosh, M. Liana, K. Rakesh, Redistribution of activated caspase-3 to the nucleus during butyric acid-induced apoptosis, Biochem. Biophys. Res. Commun. 260 (1999) 775–780.
[25] N. Li, K. Ragheb, G. Lawler, J. Sturgis, B. Rajwa, J.A. Melendez, J.P. Robinson, Mitochondrial complex I inhibitor rotenone induces apoptosis through enhancing mitochondrial reactive oxygen species production, J. Biol. Chem. 278 (2003) 8516–8525.
[26] S. Fields, A novel geneic system to detect protein–protein interactions, Nature 340 (1989) 245–246.
[27] B.A. Pollok, Using GFP in FRET-based applications, Trends Cell Biol. 9 (1999) 57–60.
[28] F. Gaits, K. Hahn, Shedding light on cell signaling: interpretation of FRET biosensors, Sci. STKE 3 (2003) 1–5.
[29] T. Kiwamu, N. Takeharu, M. Atsushi, M. Masayuki, Spatio-temporal activation of caspase revealed by indicator that is insensitive to environmental effects, J. Cell Biol. 160 (2003) 235–243.
[30] L. Tyas, V.A. Brophy, A. Pope, A.J. Rivett, J.M. Tavare, Rapid caspase-3 activation during apoptosis revealed using fluorescence-resonance energy transfer, Eur. Mol. Biol. Org. Rep. 1 (2000) 266–270.
[31] D.J. Granville, C.M. Carthy, H. Jiang, J.G. Levy, B.M. McManus, J.Y. Martroule, J. Piette, D.W.C. Hunt, Nuclear factor-κB avtivation by photochemotherapeutic agent verteporin, Immunobiology 95 (2000) 256–262.
[32] J. Moan, K. Berg, Photochemotherapy of cancer: experimental research, Photochem. Photobiol. 55 (1992) 931–948.
[33] R.U. Jänicke, M.L. Sprengart, M.R. Wati, A.G. Porter, Caspase-3 is required for DNA fragmentation and morphological changes associated with apoptosis, J. Biol. Chem. 273 (1998) 9357–9360.
[34] J.M. Chandler, G.M. Cohen, M. MacFarlane, Different subcellular distribution of caspase-3 and caspase-7 following Fas-induced apoptosis in mouse liver, J. Biol. Chem. 273 (1998) 10815–10818.
[35] B. Zhivotovsky, A. Samali, A. Gahm, S. Orrenius, Caspases: their intracellular localization and translocation during apoptosis, Cell Death Differ. 6 (1999) 644–651.
[36] M. Mahitosh, M. Liana, K. Rakesh, Redistribution of activated caspase-3 to the nucleus during butyric acid-induced apoptosis, Biochem. Biophys. Res. Commun. 260 (1999) 775–780.
[37] M.P. Boldin, T.M. Goncharov, Y.V. Goltsev, D. Wallach, Involvement of MACH, a novel MORT1/FADD-interacting protease, in Fas/APO-1-and TNF receptor-induced cell death, Cell 85 (1996) 803–815.
[38] N.L. Oleinick, R.L. Morris, I. Belichenko, The role of apoptosis in response to photodynamic therapy: what, where, why, and how, Photochem. Phtobiol. Sci. 1 (2002) 1–21.
[39] N.P. Mahajan, K. Linder, G. Berry, G.W. Gordon, R. Heim, B. Herman, Bcl-2 and Bax interactions in mitochondria probed with green fluorescent protein and fluorescence resonance energy transfer, Nat. Biotechnol. 16 (1998) 547–552.
[40] A. Miyawaki, J. Llopis, R. Heim, J.M. McCaffery, J.A. Adams, M. Ikura, R.Y. Tsien, Fluorescent indicators for Ca2+ based on green fluorescent proteins and calmodulin, Nature 388 (1997) 882–887.
[41] H. Mizuno, A. Sawano, P. Eli, H. Hama, A. Miyawaki, Red fluorescent protein from Discosoma as a fusion tag and a partner for fluorescence resonance energy transfer, Biochemistry 40 (2001) 2502–2510.
[42] J. Thorburn, L.M. Bender, M.J. Morgan, A. Thorburn, Caspase- and serine protease-dependent apoptosis by the death domain of FADD in normal epithelial cells, Mol. Biol. Cell 14 (2003) 67–77.
[43] N. Rampino, H. Yamamoto, Y. Ionov, Y. Li, H. Sawai, J.C. Reed, M. Perucho, Somatic frameshift mutations in

the BAX gene in colon cancers of the microsatellite mutator phenotype, Science 275 (1997) 967–969.
[44] C. Yin, C.M. Knudson, S.J. Korsmeyer, T. Van Dyke, Bax suppresses tumorigenesis and stimulates apoptosis in vivo, Nature 385 (1997) 637–640.
[45] Z.N. Oltvai, C.L. Milliman, S.J. Korsmeyer, Bcl-2 heterodimerizes in vivo with a conserved homolog, Bax, that accelerates programmed cell death, Cell 74 (1993) 609–619.
[46] A. Miyawaki, O. Griesbeck, R. Heim, R.Y. Tsien, Dynamic and quantitative Ca^{2+} measurements using improved cameleons, Proc. Natl Acad. Sci. USA 96 (1999) 2135–2140.
[47] A. Miyawaki, R.Y. Tsien, Monitoring protein conformations and interactions by fluorescence resonance energy transfer between mutants of green fluorescent protein, Methods Enzymol. 327 (2000) 472–500.